

# Generating large disordered stealthy hyperuniform systems with ultrahigh accuracy to determine their physical properties

Peter K. Morse ,<sup>1,2,3,\*</sup> Jaeuk Kim ,<sup>1,2,3</sup> Paul J. Steinhardt ,<sup>2</sup> and Salvatore Torquato ,<sup>1,2,4,3,5,†</sup>

<sup>1</sup>Department of Chemistry, Princeton University, Princeton, New Jersey 08544, USA

<sup>2</sup>Department of Physics, Princeton University, Princeton, New Jersey 08544, USA

<sup>3</sup>Princeton Institute of Materials, Princeton University, Princeton, New Jersey 08544, USA

<sup>4</sup>Princeton Center for Theoretical Science, Princeton University, Princeton, New Jersey 08544, USA

<sup>5</sup>Program in Applied and Computational Mathematics, Princeton University, Princeton, New Jersey 08544, USA



(Received 19 April 2023; accepted 28 August 2023; published 15 September 2023)

Hyperuniform many-particle systems are characterized by a structure factor  $S(\mathbf{k})$  that is precisely zero as  $|\mathbf{k}| \rightarrow 0$ ; and stealthy hyperuniform systems have  $S(\mathbf{k}) = 0$  for the finite range  $0 < |\mathbf{k}| \leq K$ , called the “exclusion region.” Through a process of collective-coordinate optimization, energy-minimizing disordered stealthy hyperuniform systems of moderate size have been made to high accuracy, and their novel physical properties have shown great promise. However, minimizing  $S(\mathbf{k})$  in the exclusion region is computationally intensive as the system size becomes large. In this paper, we present an improved methodology to generate such states using double-double precision calculations on graphical processing units (GPUs) that reduces the deviations from zero within the exclusion region by a factor of approximately  $10^{30}$  for system sizes more than an order of magnitude larger. We further show that this ultrahigh accuracy is required to draw conclusions about their corresponding characteristics, such as the nature of the associated energy landscape and the presence or absence of Anderson localization, which might be masked, even when deviations are relatively small.

DOI: [10.1103/PhysRevResearch.5.033190](https://doi.org/10.1103/PhysRevResearch.5.033190)

## I. INTRODUCTION

Disordered hyperuniform systems are isotropic like a glass but have long-range correlations that result in the anomalous suppression of density fluctuations over large distances [1]. This feature endows them with unique physical properties not possible in ordered (periodic or quasiperiodic) systems [2–5]. The disordered varieties include perfect glasses, fermionic point processes, disordered jammed particle packings, quantum states, certain plasmas, galaxy distributions, eigenvalues of random matrices, and myriad other examples (see Ref. [6] and references therein).

A defining feature of a disordered hyperuniform system in  $d$ -dimensional Euclidean space  $\mathbb{R}^d$ , aside from its isotropy, is that the structure factor  $S(\mathbf{k})$  vanishes as the wave number  $k \equiv |\mathbf{k}|$  tends to zero [1,6]. An important subclass is the *stealthy* disordered hyperuniform system in which  $S(\mathbf{k}) = 0$  for a finite range of wave numbers  $0 < k \leq K$ . This range defines the *exclusion region* in Fourier space where no single-scattering events can occur [7–10], leading to them being theoretically analyzed as  $d$ -dimensional “hard-sphere fluids” in Fourier space [10]. Disordered stealthy hyperuniform systems stand

out among all nonstealthy hyperuniform ones because they anomalously suppress density fluctuations not only at infinite wavelengths but down to intermediate wavelengths [6]. Moreover, “holes” in any disordered stealthy hyperuniform point pattern are strictly bounded with a well-defined maximal size in the thermodynamic limit [6,11,12]. All of these remarkable attributes are responsible for the novel wave, transport, and mechanical properties of disordered stealthy hyperuniform systems [6]. For example, a scheme that maps stealthy hyperuniform point patterns onto disordered dielectric networks resulted in the first moderately sized amorphous photonic solid samples with complete photonic band gaps comparable to those in periodic networks with the advantage that the band gaps are isotropic [13]. Since this work, disordered stealthy systems have been extensively fabricated [2,4,14–28] and studied computationally especially due to their novel optical [2,15,18,20–22], photonic [4,14,17,19,28], electronic [29,30], phononic [23–26], and transport [16,27] properties.

Since hyperuniformity is a large-scale property of a system, it is imperative to be able to generate sample sizes much larger than those presently possible [31] in order to ascertain whether their novel properties persist as the sample size becomes large. Indeed, this question was recently explored in the context of photonics, where numerical evidence was presented to show that among various disordered nonhyperuniform and hyperuniform dielectric network solids, only certain stealthy hyperuniform ones may form band gaps in the thermodynamic limit [28]. Importantly, the band gaps for networks with near stealthiness [small but positive  $S(\mathbf{k})$  within the exclusion region] eventually closed as the system size grew with a rate inversely proportional to the *distance to*

\*Corresponding author: peter.k.morse@gmail.com

†Corresponding author: torquato@princeton.edu

Published by the American Physical Society under the terms of the [Creative Commons Attribution 4.0 International](https://creativecommons.org/licenses/by/4.0/) license. Further distribution of this work must maintain attribution to the author(s) and the published article's title, journal citation, and DOI.

stealthiness  $S_{\max}$ , which we define in the present work as

$$S_{\max} \equiv \max_{0 < k \leq K} S(\mathbf{k}). \quad (1)$$

The work reported in Ref. [28] emphasizes the importance of computationally creating appreciably larger disordered stealthy hyperuniform systems, but ones with the smallest value of  $S_{\max}$  within the exclusion region.

Remarkably, disordered stealthy hyperuniform point patterns are highly degenerate ground states for certain nontrivial oscillatory pair potentials (see Ref. [10] and references therein). Such ground states have been generated using a collective-coordinate energy optimization scheme [7,9,32,33]. As such, they inevitably have a small positive residual  $S(\mathbf{k})$  in the exclusion region, i.e., small  $S_{\max}$ , due to the level of precision with which they were prepared. In dimensions  $d = 1-3$ , the largest simulated disordered stealthy hyperuniform systems have had  $N = 10^3, 10^4$ , and  $8 \times 10^3$  particles, respectively [34], and the highest accuracy achieved has been  $S_{\max} \approx 10^{-22}$  [33]. In order to extrapolate reliably to the thermodynamic limit, significantly larger systems with a small  $S_{\max}$  are required. However, the computational cost of the standard collective-coordinate minimization schemes scales as at least  $O(N^2)$  (derived in Sec. III), making it nearly impossible to reach the requirements without fundamentally modifying the procedure.

In this paper, we show that the collective-coordinate minimization is highly parallelizable and requires very little memory access, making it ideally suited for a GPU (graphical processing unit)-based algorithm. The high degree of parallelization afforded by GPUs allows us to create systems 20 times larger than previous best efforts [34] in comparable time and with  $S_{\max}$  reduced by 30 orders of magnitude, i.e.,  $S_{\max} \approx 10^{-51}$ . This enables us to study the energy landscape associated with the stealthy hyperuniform potential and lays the groundwork for extrapolations to both the thermodynamic and high- $d$  limits. While the techniques used are independent of dimension, we focus on  $d = 2$  with system size  $N = 2 \times 10^6$  as a trial case for its ease of representation.

Moreover, we show the importance of creating states with the smallest  $S_{\max}$  by showing that values of  $S_{\max}$  which were deemed relatively small in the past can still vastly degrade certain desired physical properties. For each application, it is then necessary to ask what level of  $S_{\max}$  is sufficient. In particular, we show that for two-dimensional (2D) two-phase media derived from stealthy hyperuniform point patterns, a full transparency interval for light propagation in which there is no Anderson localization depends on having  $S_{\max}$  precisely zero over the exclusion region. Thus, the ability to generate stealthy hyperuniform systems over an exponentially wide range of  $S_{\max}$  is essential for extrapolating to the thermodynamic limit. This high precision is also necessary to understand key properties of the ground-state manifold of the stealthy hyperuniform potential—namely its connectivity and dimension—especially near critical points.

## II. DEFINITIONS

The collective-coordinate method for generating disordered stealthy hyperuniform point patterns is based on finding

the ground state for a system of point particles whose total potential energy is the sum of pairwise potentials  $v(\mathbf{r})$ , where  $v(\mathbf{r})$  is bounded and integrable such that its Fourier transform  $\tilde{v}(\mathbf{k})$  exists and is a positive function with compact support over the interval  $0 < |\mathbf{k}| \leq K$ . Given a set of  $N$  points at positions  $\mathbf{r}_j$  within a periodic box  $F$  of volume  $v_F$  in  $\mathbb{R}^d$ . The total potential energy  $\Phi(\mathbf{r}^N)$  has the Fourier representation [10]

$$\Phi(\mathbf{r}^N) = \frac{N}{2v_F} \left[ \sum_{0 < k \leq K} \tilde{v}(\mathbf{k}) S(\mathbf{k}) - \sum_{0 < k \leq K} \tilde{v}(\mathbf{k}) \right], \quad (2)$$

where  $S(\mathbf{k})$  is the structure factor of a *single* configuration defined by

$$S(\mathbf{k}) = \frac{|\tilde{n}(\mathbf{k})|^2}{N}, \quad (3)$$

where  $\mathbf{k}$  is a nonzero reciprocal lattice vector of  $F$ , and  $\tilde{n}(\mathbf{k})$  is the complex collective density variable given by

$$\tilde{n}(\mathbf{k}) = \sum_{j=1}^N \exp(-i\mathbf{k} \cdot \mathbf{r}_j). \quad (4)$$

The second term in (2) is structure independent, and so we drop it. The potential  $\Phi$  is thus bounded from below by  $\Phi = 0$ , which defines the ground-state manifold within which all states are stealthy hyperuniform. Note that because  $\tilde{v}(\mathbf{k})$  is strictly positive, it does not modify the definition of the ground-state manifold, though it does provide a weight function that will funnel any dynamic or thermal processes on the  $\Phi$  landscape towards specific ground states [33].

The periodic hypercubic box has side length  $L$ , and all  $k$  vectors form a hypercubic lattice of lattice spacing  $2\pi/L$ , meaning one can count the number of unique  $k$  vectors for which  $0 < k \leq K$ . Because the structure factor has inversion symmetry, i.e.,  $S(\mathbf{k}) = S(-\mathbf{k})$ , if there were  $(2M + 1)$  vectors for which  $0 < k \leq K$ , then only  $M$  are independent. The parameter  $\chi$  measures the fraction of degrees of freedom constrained relative to the total of  $d(N - 1)$  degrees of freedom in a  $d$ -dimensional point pattern, i.e.,

$$\chi = \frac{M}{d(N - 1)}. \quad (5)$$

Ground states with  $\chi \geq 1/2$  in  $d \leq 4$  always form ordered hyperuniform structures, and so we restrict ourselves here to  $\chi < 1/2$  in  $d = 2$ . Results for other dimensions will be reported elsewhere.

The energy landscape for the stealthy hyperuniform potential in the disordered regime ( $\chi < 1/2$  in  $d > 1$  or  $\chi < 1/3$  in  $d = 1$ ) is simple. Previous studies have shown that the *inherent structure* for any initial condition—defined as the nearest local energy minimum accessible without a barrier crossing [36]—is itself one of the many degenerate global minima [7–9,33]. Thus, a simple quench, achieved via standard local energy minimization methods, generically yields a ground state. While previous studies found this to be true to an arbitrarily assigned threshold  $\Phi < 10^{-22}$  [33], this finding will be verified to greater accuracy in this work.

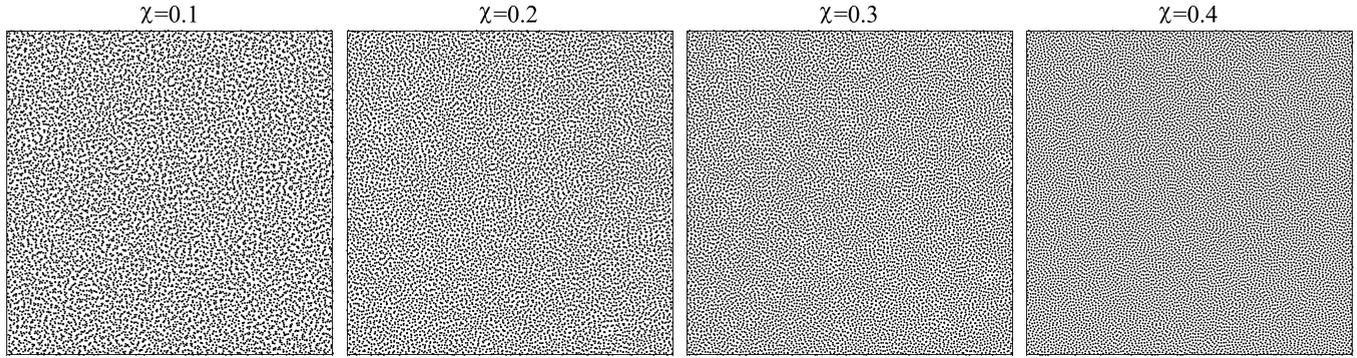


FIG. 1. Stealthy hyperuniform point patterns of  $N = 2 \times 10^6$  particles with  $\chi = 0.1, 0.2, 0.3,$  and  $0.4$ . Each image only shows  $1/16$ th of all the data for better visualizations. Full configuration data are deposited through Princeton Data Commons [35].

### III. SIMULATIONS

Generating disordered stealthy hyperuniform systems involves finding true ground states of  $\Phi$  in Eq. (2). When  $\chi < 1/2$ , the disordered ground states are infinitely degenerate in the thermodynamic limit [10]. Both the initial conditions and the choice of  $\tilde{v}(\mathbf{k})$  affect the particular ground state obtained [33]. For the purposes of illustration, we use random initial conditions defined by a Poisson point process and  $\tilde{v}(\mathbf{k}) = \varepsilon_0 L^d \Theta(K - k)$ , where  $\Theta(x)$  is the Heaviside function and  $\varepsilon_0$  sets the units of energy.

To minimize Eq. (2), we need its value and the gradient

$$\mathbf{F}_j = -\nabla_j \Phi(\mathbf{r}^N) = \frac{1}{v_F} \sum_{0 < k \leq K} \mathbf{k} \tilde{v}(\mathbf{k}) \text{Im}[\tilde{n}(\mathbf{k}) \exp(i\mathbf{k} \cdot \mathbf{r}_j)], \quad (6)$$

which is another input of a minimizer. Here, we use the fast inertial relaxation engine (FIRE) minimization [37], because

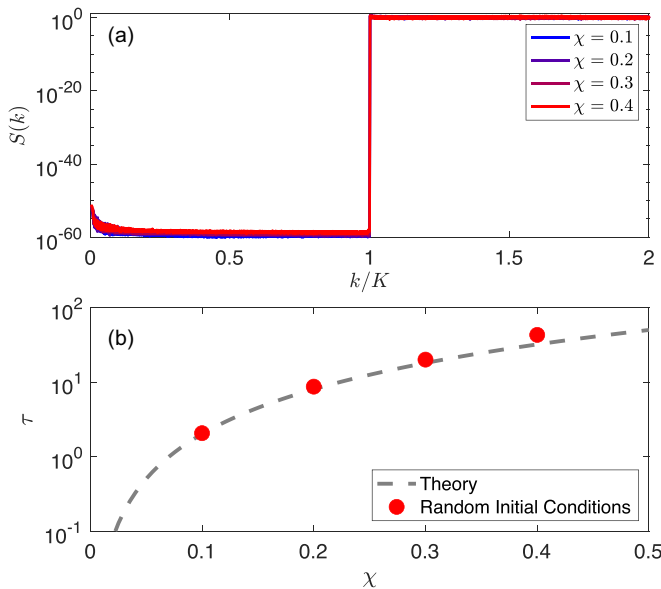


FIG. 2. (a) The structure factor, after optimization, yields  $S_{\max} \approx 10^{-51}$ . (b) The order metric  $\tau$  plotted as a function of  $\chi$  for the simulation data (red circles) compared to the theoretical curve for entropically favored states [10].

it requires fewer computations and converges faster than comparable minimizers.

By far, the most computationally expensive quantity of the minimization is the gradient, which contains two sums. First, one calculates all  $M$  independent values of  $\tilde{n}(\mathbf{k})$ , each of which contains  $N$  terms. Then, one must calculate the gradient for all  $N$  particles, each of which contains a sum over  $M$  terms. Each of these calculations involves  $MN = \chi N(N - 1)d$  terms and needs to be recalculated at every step of the minimization, setting the minimum timescale for minimization as  $O(N^2)$ . The substantial numerical speedup comes from the realization that both Eqs. (4) and (6) are simple parallel reduction sums, which are ideally suited for GPUs. To implement these quenches, we use the GPU-based packing software pyCudaPack [38–44], because of its highly optimized modular implementation of a variety of pair interactions [38,39,43,44] using various minimizers [39] on double-doubles [40–42]. Minimizations proceed until  $\Phi$  is at the minimum value attainable within machine precision, which for  $N = 2 \times 10^6$  is  $\Phi/\varepsilon_0 \approx 10^{-46}$ . These are thus ground states to within double-double numerical precision.

It is well established that short- and intermediate-range order increase with the size of the exclusion region between  $\chi = 0$  and  $1/2$  in  $d = 2$  [7–10,33]. A positive order metric that measures the degree to which translational order increases with  $\chi$  across length scales is [10]

$$\tau \equiv \frac{1}{D^d} \int_{\mathbb{R}^d} h^2(r) d\mathbf{r} = \frac{1}{(2\pi D)^d \rho^2} \int_{\mathbb{R}^d} [S(\mathbf{k}) - 1]^2 d\mathbf{k}, \quad (7)$$

where  $\rho$  is the number density,  $h(r)$  is the total correlation function [45],  $S(\mathbf{k})$  is the ensemble average of Eq. (3) in the thermodynamic limit, and  $D$  is a characteristic length scale, taken as  $D = K^{-1}$ . For an ideal gas (spatially uncorrelated Poisson point process),  $\tau = 0$  because  $h(r) = 0$  for all  $r$ . Thus, a deviation of  $\tau$  from zero measures translational order with respect to the fully uncorrelated case. While  $\tau$  diverges for perfect crystals and quasicrystals in the infinite-system limit, its rate of growth as a function of system size still provides a useful measure of the translational order in such ordered systems [46,47].

#### IV. RESULTS AND DISCUSSION

We create five disordered stealthy hyperuniform systems in  $d = 2$  at each value of  $\chi = 0.1, 0.2, 0.3,$  and  $0.4$  to demonstrate the ultrahigh accuracy of our GPU-based algorithm. Our results have both high precision—in that they are done using double-doubles—and high accuracy, as measured by exceptionally small values of  $S_{\max}$ . Figure 1 shows one system at each value of  $\chi$ . To demonstrate the level of accuracy, we plot the structure factor on a logarithmic scale [Fig. 2(a); see Fig. 4 in the Appendix for the linear scale]. Here,  $S_{\max}$  depends explicitly on the form of  $\tilde{v}(\mathbf{k})$ , with our particular choice yielding  $S_{\max} = S(k_{\min})$ .

While  $S(k > K)$  depends strongly on initial temperature [33], in Fig. 2(b) we find that the theoretical curve for  $\tau$  derived for low-temperature initial states departs by relatively small amounts compared to the data obtained from high-temperature states (i.e., random initial conditions). This implies that while the respective pointwise behaviors of the pair correlation function and  $S(\mathbf{k})$  may sometimes differ for certain small ranges of their arguments, the integrated measure of order across length scales for stealthy hyperuniform states from low- $T$  and high- $T$  initial states, as measured by  $\tau$ , are essentially the same. Whether this remains true in other dimensions is a subject for future work.

We now vividly demonstrate the importance of small  $S_{\max}$  by mapping stealthy hyperuniform patterns into two-phase dielectric media and quantifying the attenuation of electromagnetic waves propagating through them. Specifically, we map 2D stealthy hyperuniform point patterns that are exactly stealthy (i.e.,  $S_{\max} = 0$ ) in the thermodynamic limit via theoretical methods described in Ref. [10] into a distribution of disks (phase 2) of dielectric constant  $\varepsilon_2 = 1$  in a matrix (phase 1) of dielectric constant  $\varepsilon_1 = 11.6$  by circumscribing each point with identical disks of radius  $a$  without overlap [16,48,49]. The resulting area fraction covered by disks is  $\phi_2 = 0.112$ . By a similar analysis, we allow  $S_{\max}$  to be a free parameter. The *spectral density*  $\tilde{\chi}_V(k)$  of these disks is computed from the formula [49]  $\tilde{\chi}_V(k) = 4\pi\phi_2[J_1(ka)/k]^2 S(k)$ , where  $J_1(x)$  is the Bessel function of the first kind of order 1. The resulting  $\tilde{\chi}_V(k)$  is valid in the thermodynamic limit and inherits the distance to stealthiness  $S_{\max}$  of the original point patterns, in which  $S_{\max}$  is either exactly zero or a specified positive value [50]; see Fig. 3(a). We obtain the effective dynamic dielectric constant  $\varepsilon_e^{\text{TE}}(k_1)$  of such two-phase media for incident light of transverse electric (TE) polarization and wave number  $k_1$  by using a nonlocal strong-contrast approximation [see Eq. (73) for  $d = 2$  in Ref. [51]] that depends on  $\tilde{\chi}_V(k)$ , which accurately captures multiple scattering effects to all orders beyond the quasistatic regime (i.e.,  $0 \leq k_1\xi \lesssim 1$ , where  $\xi$  is a characteristic inhomogeneity length scale).

The key property of interest here in this system is the imaginary part of  $\varepsilon_e^{\text{TE}}(k_1)$  which measures the degree to which the media effectively attenuate light, as shown in Fig. 3(b). Importantly, perfect stealthy hyperuniform media with  $S_{\max} = 0$  exhibit full transparency (i.e.,  $\text{Im}[\varepsilon_e^{\text{TE}}(k_1)] = 0$ ) up to a finite wave number in the thermodynamic limit, implying the absence of Anderson localization [52–54]. By contrast, a stealthy hyperuniform medium with a moderate distance

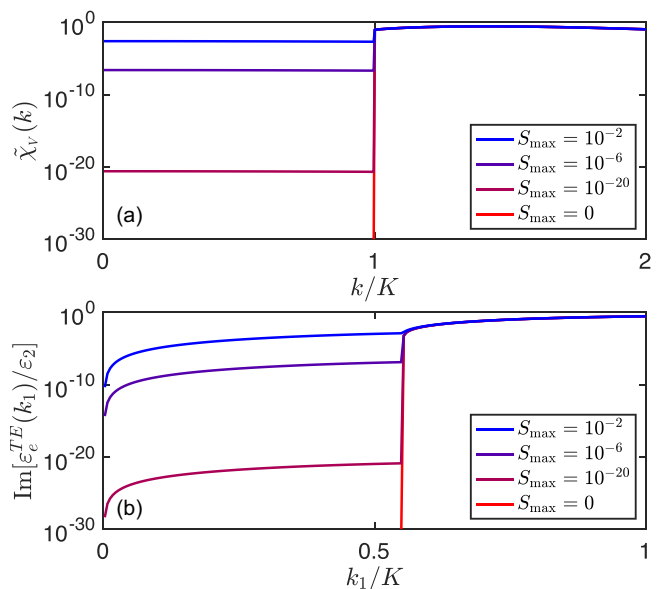


FIG. 3. 2D media consisting of packings of identical disks of dielectric constant  $\varepsilon_2 = 1$  and packing fraction  $\phi_2 = 0.112$  in a matrix of dielectric constant  $\varepsilon_1 = 11.6$ . The disk centers have  $S(k) = S_{\max}$  in the exclusion region ( $k \leq K$ ). (a) Semilog plot of the spectral density  $\tilde{\chi}_V(k)$  as a function of a dimensionless wave number  $k/K$ . (b) Semilog plot of the imaginary part of the effective dynamic dielectric constant  $\text{Im}[\varepsilon_e^{\text{TE}}(k_1)]$  for transverse electric (TE) polarization vs the dimensionless incident wave number  $k_1/K$  in phase 1. While the presence of the transparency regime is independent of  $\chi$ , for illustration we have chosen  $\chi = 0.4$ .

to stealthiness ( $0 \ll S_{\max} < 1$ ) has a positive  $\text{Im}[\varepsilon_e^{\text{TE}}(k_1)]$  proportional to  $S_{\max}$  up to  $k_1 = O(K)$ , implying that transmittance through this medium is increasingly suppressed with a larger sample size or a larger  $S_{\max}$ , and that Anderson localization likely emerges. Thus, to better understand the insulator-conductor transition as the system size increases, it is essential to generate much larger samples with a small  $S_{\max}$  via the techniques described here.

#### V. CONCLUSIONS

Through the use of GPU minimizations with double-double precision, we are able to dramatically increase the size and reduce the distance to stealthiness of stealthy hyperuniform point patterns. The ability to create disordered stealthy hyperuniform systems of both large sizes and ultrasmall  $S_{\max}$  is imperative to study their novel properties. While the requirement for large sample sizes has been recognized, the need for a small  $S_{\max}$  has gone largely unnoticed due to the inability to create large samples. Indeed, most previous studies were based on relatively small sample sizes ( $100 \lesssim N \lesssim 1000$ ) with  $10^{-10} \lesssim S_{\max} \lesssim 10^{-5}$ . A capacity to create much larger systems with very small values of  $S_{\max}$  can shed light on the emerging novel properties of stealthy hyperuniform systems that depend on having a small distance to stealthiness. One such open question is whether isotropic photonic (or phononic) band gaps exist in two-phase systems derived from stealthy hyperuniform point patterns in the thermodynamic limit [28]. In addition, while disordered

stealthy hyperuniform systems of moderate sizes are known to be transparent up to a finite  $k$  for electromagnetic [15,17,51] and elastic waves [21,25,26], it is not known whether this transparency interval persists in the thermodynamic limit. If it does persist, this implies no Anderson localization. Our theoretical analysis [summarized in Fig. 3(b)] shows that this transparency property increasingly degrades as  $S_{\max}$  and the system size are made larger, stressing the importance of making  $S_{\max}$  for a given system as small as possible, which is now achieved with ultrahigh accuracy via our improved numerical methodology. Samples of much larger size with vastly smaller  $S_{\max}$  can now be potentially fabricated by combining our designs with photolithographic and 3D printing techniques [55–57] to explore the presence or absence of Anderson localization [52,53,58] in disordered stealthy hyperuniform systems as a function of sample size.

These high-precision results also lay the groundwork for further characterization of the energy landscape of the stealthy hyperuniform potential. Indeed, we now have abundant evidence that local minima do not exist (or are extremely rare) for  $\chi < 1/2$ , implying that states with high values of  $S_{\max}$  found in previous studies are not locally stable; rather, they are the result of incomplete minimization, making them excited states with an effective positive temperature and a modified isothermal compressibility [10]. Future work will aim to characterize the ground-state manifold, particularly its connectivity, the topology near crystalline states, and the topological change that occurs when  $\chi = 1/2$  (especially as a function of dimension) and how these landscape properties modify the physical properties of disordered stealthy hyperuniform systems. Moreover, with larger systems, one will be able to probe higher-order correlation functions beyond  $\tau$  in determining the structural order in stealthy hyperuniform systems [34]. Additionally, while we have focused here on isotropic exclusion regions, it is straightforward to generalize to anisotropic exclusion regions, and thus statistically anisotropic ground states [59,60].

#### ACKNOWLEDGMENTS

The research was sponsored by the U.S. Army Research Office and was accomplished under Cooperative Agreement No. W911NF-22-2-0103. Simulations were performed on computational resources managed and supported by the Princeton Institute for Computational Science and Engineering (PICSciE). P.K.M. would like to thank Eric Corwin for discussions related to pyCudaPack.

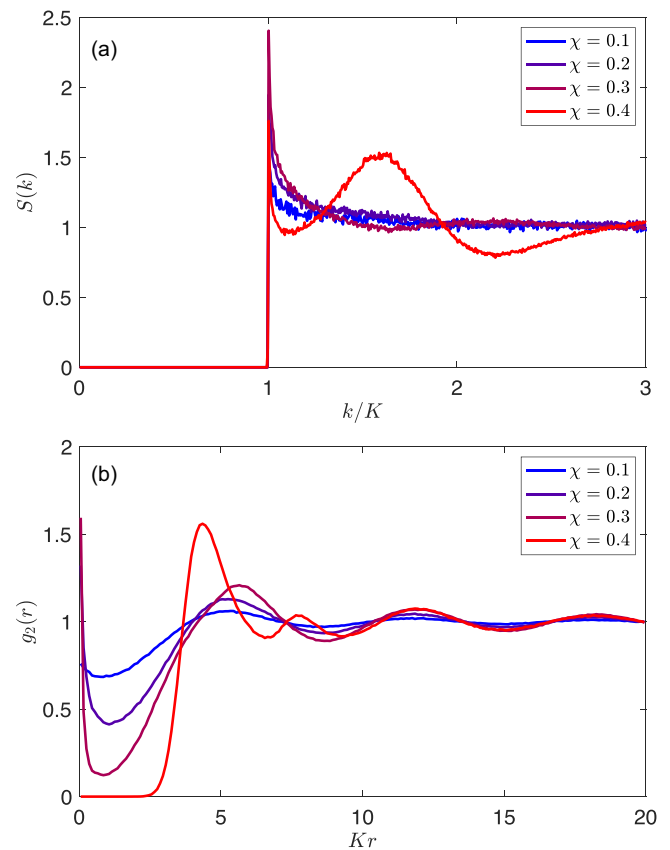


FIG. 4. (a) Data from Fig. 2 plotted on a linear scale. (b) The pair correlation function  $g_2(r)$  for the same set of data. Note here the exclusion region forming for low  $r$  as  $\chi$  increases. Length scales are set by the choice  $K = 1$ . Both (a) and (b) are consistent with Fig. 1 of Ref. [33]

#### APPENDIX: PAIR CORRELATION FUNCTION AND STRUCTURE FACTOR

In Fig. 2, the structure factor was shown on a semilog scale in order to demonstrate the level of accuracy achieved in creating stealthy hyperuniform systems with a minimal  $S_{\max}$ . Here, in Fig. 4(a), it is shown on the more familiar linear scale. Also included is a plot of the pair correlation function  $g_2(r)$ ; see Fig. 4(b). As noted throughout the text, this data set is taken from random initial conditions and thus does not follow the predictions for entropically favored states shown in Ref. [10]. Instead, it should be compared to Fig. 1 of Ref. [33], with which it is entirely consistent.

- [1] S. Torquato and F. H. Stillinger, Local density fluctuations, hyperuniformity, and order metrics, *Phys. Rev. E* **68**, 041113 (2003).
- [2] B.-Y. Wu, X.-Q. Sheng, and Y. Hao, Effective media properties of hyperuniform disordered composite materials, *PLoS One* **12**, e0185921 (2017).
- [3] M. Salvalaglio, M. Bouabdellaoui, M. Bollani, A. Benali, L. Favre, J.-B. Claude, J. Wenger, P. de Anna, F. Intonti, A. Voigt,

and M. Abbarchi, Hyperuniform Monocrystalline Structures by Spinodal Solid-State Dewetting, *Phys. Rev. Lett.* **125**, 126101 (2020).

- [4] S. Yu, C.-W. Qiu, Y. Chong, S. Torquato, and N. Park, Engineered disorder in photonics, *Nat. Rev. Mater.* **6**, 226 (2021).
- [5] S. Yu, Evolving scattering networks for engineering disorder, *Nat. Comput. Sci.* **3**, 128 (2023).

- [6] S. Torquato, Hyperuniform states of matter, *Phys. Rep.* **745**, 1 (2018).
- [7] O. U. Uche, F. H. Stillinger, and S. Torquato, Constraints on collective density variables: Two dimensions, *Phys. Rev. E* **70**, 046122 (2004).
- [8] O. U. Uche, S. Torquato, and F. H. Stillinger, Collective coordinate control of density distributions, *Phys. Rev. E* **74**, 031104 (2006).
- [9] R. D. Batten, F. H. Stillinger, and S. Torquato, Classical disordered ground states: Super-ideal gases and stealth and equi-luminous materials, *J. Appl. Phys.* **104**, 033504 (2008).
- [10] S. Torquato, G. Zhang, and F. H. Stillinger, Ensemble Theory for Stealthy Hyperuniform Disordered Ground States, *Phys. Rev. X* **5**, 021020 (2015).
- [11] G. Zhang, F. H. Stillinger, and S. Torquato, Can exotic disordered “stealthy” particle configurations tolerate arbitrarily large holes? *Soft Matter* **13**, 6197 (2017).
- [12] S. Ghosh and J. L. Lebowitz, Generalized stealthy hyperuniform processes: Maximal rigidity and the bounded holes conjecture, *Commun. Math. Phys.* **363**, 97 (2018).
- [13] M. Florescu, S. Torquato, and P. J. Steinhardt, Designer disordered materials with large, complete photonic band gaps, *Proc. Natl. Acad. Sci. USA* **106**, 20658 (2009).
- [14] W. Man, M. Florescu, E. P. Williamson, Y. He, S. R. Hashemizad, B. Y. C. Leung, D. R. Liner, S. Torquato, P. M. Chaikin, and P. J. Steinhardt, Isotropic band gaps and freeform waveguides observed in hyperuniform disordered photonic solids, *Proc. Natl. Acad. Sci. USA* **110**, 15886 (2013).
- [15] O. Leseur, R. Pierrat, and R. Carminati, High-density hyperuniform materials can be transparent, *Optica* **3**, 763 (2016).
- [16] G. Zhang, F. H. Stillinger, and S. Torquato, Transport, geometrical, and topological properties of stealthy disordered hyperuniform two-phase systems, *J. Chem. Phys.* **145**, 244109 (2016).
- [17] L. S. Froufe-Pérez, M. Engel, J. J. Sáenz, and F. Scheffold, Band gap formation and Anderson localization in disordered photonic materials with structural correlations, *Proc. Natl. Acad. Sci. USA* **114**, 9570 (2017).
- [18] D. Chen and S. Torquato, Designing disordered hyperuniform two-phase materials with novel physical properties, *Acta Mater.* **142**, 152 (2018).
- [19] S. Gorsky, W. A. Britton, Y. Chen, J. Montaner, A. Lenef, M. Raukas, and L. Dal Negro, Engineered hyperuniformity for directional light extraction, *APL Photonics* **4**, 110801 (2019).
- [20] A. Sheremet, R. Pierrat, and R. Carminati, Absorption of scalar waves in correlated disordered media and its maximization using stealth hyperuniformity, *Phys. Rev. A* **101**, 053829 (2020).
- [21] J. Kim and S. Torquato, Multifunctional composites for elastic and electromagnetic wave propagation, *Proc. Natl. Acad. Sci. USA* **117**, 8764 (2020).
- [22] N. Tavakoli, R. Spalding, A. Lambertz, P. Koppejan, G. Gkantzounis, C. Wan, R. Röhrich, E. Kontoleta, A. F. Koenderink, R. Sapienza, M. Florescu, and E. Alarcon-Llado, Over 65% sunlight absorption in a 1  $\mu\text{m}$  Si slab with hyperuniform texture, *ACS Photonics* **9**, 1206 (2022).
- [23] G. Gkantzounis, T. Amoah, and M. Florescu, Hyperuniform disordered phononic structures, *Phys. Rev. B* **95**, 094120 (2017).
- [24] V. Romero-García, N. Lamothe, G. Theocharis, O. Richoux, and L. M. García-Raffi, Stealth Acoustic Materials, *Phys. Rev. Appl.* **11**, 054076 (2019).
- [25] A. Rohfritsch, J. M. Conoir, T. Valier-Brasier, and R. Marchiano, Impact of particle size and multiple scattering on the propagation of waves in stealthy-hyperuniform media, *Phys. Rev. E* **102**, 053001 (2020).
- [26] V. Romero-García, É. Chéron, S. Kuznetsova, J.-P. Groby, S. Félix, V. Pagneux, and L. M. García-Raffi, Wave transport in 1D stealthy hyperuniform phononic materials made of non-resonant and resonant scatterers, *APL Mater.* **9**, 101101 (2021).
- [27] É. Chéron, S. Félix, J.-P. Groby, V. Pagneux, and V. Romero-García, Wave transport in stealth hyperuniform materials: The diffusive regime and beyond, *Appl. Phys. Lett.* **121**, 061702 (2022).
- [28] M. A. Klatt, P. J. Steinhardt, and S. Torquato, Wave propagation and band tails of two-dimensional disordered systems in the thermodynamic limit, *Proc. Natl. Acad. Sci. USA* **119**, e2213633119 (2022).
- [29] S. Torquato and D. Chen, Multifunctional hyperuniform cellular networks: Optimality, anisotropy and disorder, *Multifunct. Mater.* **1**, 015001 (2018).
- [30] N. Granchi, R. Spalding, M. Lodde, M. Petruzzella, F. W. Otten, A. Fiore, F. Intonti, R. Sapienza, M. Florescu, and M. Gurioli, Near-field investigation of luminescent hyperuniform disordered materials, *Adv. Opt. Mater.* **10**, 2102565 (2022).
- [31] G. Zhang and S. Torquato, Realizable hyperuniform and non-hyperuniform particle configurations with targeted spectral functions via effective pair interactions, *Phys. Rev. E* **101**, 032124 (2020).
- [32] Y. Fan, J. K. Percus, D. K. Stillinger, and F. H. Stillinger, Constraints on collective density variables: One dimension, *Phys. Rev. A* **44**, 2394 (1991).
- [33] G. Zhang, F. H. Stillinger, and S. Torquato, Ground states of stealthy hyperuniform potentials: I. Entropically favored configurations, *Phys. Rev. E* **92**, 022119 (2015).
- [34] S. Torquato, J. Kim, and M. A. Klatt, Local Number Fluctuations in Hyperuniform and Nonhyperuniform Systems: Higher-Order Moments and Distribution Functions, *Phys. Rev. X* **11**, 021028 (2021).
- [35] Data and the generating code will be available after a brief embargo period through Princeton Data Commons at <https://doi.org/10.34770/e49n-r807>.
- [36] F. H. Stillinger and T. A. Weber, Packing structures and transitions in liquids and solids, *Science* **225**, 983 (1984).
- [37] E. Bitzek, P. Koskinen, F. Gähler, M. Moseler, and P. Gumbsch, Structural Relaxation Made Simple, *Phys. Rev. Lett.* **97**, 170201 (2006).
- [38] P. Charbonneau, E. I. Corwin, G. Parisi, and F. Zamponi, Universal Microstructure and Mechanical Stability of Jammed Packings, *Phys. Rev. Lett.* **109**, 205501 (2012).
- [39] P. K. Morse and E. I. Corwin, Geometric Signatures of Jamming in the Mechanical Vacuum, *Phys. Rev. Lett.* **112**, 115701 (2014).
- [40] P. Charbonneau, E. I. Corwin, G. Parisi, and F. Zamponi, Jamming Criticality Revealed by Removing Localized Buckling Excitations, *Phys. Rev. Lett.* **114**, 125504 (2015).
- [41] P. K. Morse and E. I. Corwin, Geometric order parameters derived from the Voronoi tessellation show signatures of the jamming transition, *Soft Matter* **12**, 1248 (2016).
- [42] P. K. Morse and E. I. Corwin, Echoes of the Glass Transition in Athermal Soft Spheres, *Phys. Rev. Lett.* **119**, 118003 (2017).

- [43] F. Arceri and E. I. Corwin, Vibrational Properties of Hard and Soft Spheres Are Unified at Jamming, *Phys. Rev. Lett.* **124**, 238002 (2020).
- [44] P. K. Morse, S. Roy, E. Agoritsas, E. Stanifer, E. I. Corwin, and M. L. Manning, A direct link between active matter and sheared granular systems, *Proc. Natl. Acad. Sci. USA* **118**, e2019909118 (2021).
- [45] The total correlation function  $h(r)$  is related to the pair correlation function  $g_2(r)$  as  $h(r) \equiv g_2(r) - 1$ .
- [46] S. Torquato, G. Zhang, and M. de Courcy-Ireland, Uncovering multiscale order in the prime numbers via scattering, *J. Stat. Mech.* (2018) 093401.
- [47] S. Torquato, G. Zhang, and M. D. Courcy-Ireland, Hidden multiscale order in the primes, *J. Phys. A: Math. Theor.* **52**, 135002 (2019).
- [48] In transitioning from a stealthy hyperuniform point pattern to a particle packing with a given packing fraction, particle overlaps can be prevented either by choosing a sufficiently large value of  $\chi$  [33], as done in Fig. 3(b), or by using an objective function of the form  $\Phi_{\text{tot}}(\mathbf{r}^N) = \Phi_{\text{SR}}(\mathbf{r}^N) + \Phi(\mathbf{r}^N)$ , where  $\Phi(\mathbf{r}^N)$  is the standard objective function Eq. (2) and  $\Phi_{\text{SR}}(\mathbf{r}^N)$  represents short-range interactions which can be a pairwise sum of hard-core repulsion or the positive parts of the Lennard-Jones potential such that its value is always non-negative. Then, ground states with  $\Phi_{\text{tot}} = 0$ , if they exist, should be stealthy hyperuniform without overlaps. A similar treatment can be found in Ref. [21].
- [49] S. Torquato, Disordered hyperuniform heterogeneous materials, *J. Phys.: Condens. Matter* **28**, 414012 (2016).
- [50] Since disordered stealthy hyperuniform point patterns can be treated as hard-sphere fluids in Fourier space [10],  $S(k)$  decays to unity exponentially fast. Thus, the precise form of  $S(k)$  outside the exclusion region is irrelevant for our purposes because the value of  $S(k)$  within the exclusion region determines the value of  $\text{Im}[\varepsilon_e^{\text{TE}}(k_1)]$  within the full transparency interval. For this reason, we do not present the precise form here.
- [51] S. Torquato and J. Kim, Nonlocal Effective Electromagnetic Wave Characteristics of Composite Media: Beyond the Quasi-static Regime, *Phys. Rev. X* **11**, 021002 (2021).
- [52] A. R. McGurn, K. T. Christensen, F. M. Mueller, and A. A. Maradudin, Anderson localization in one-dimensional randomly disordered optical systems that are periodic on average, *Phys. Rev. B* **47**, 13120 (1993).
- [53] C. M. Aegerter and G. Maret, Coherent backscattering and Anderson localization of light, in *Progress in Optics*, Vol. 52 (Elsevier, Amsterdam, 2009), pp. 1–62.
- [54] F. Sgrignuoli, S. Torquato, and L. Dal Negro, Subdiffusive wave transport and weak localization transition in three-dimensional stealthy hyperuniform disordered systems, *Phys. Rev. B* **105**, 064204 (2022).
- [55] J. R. Tumbleston, D. Shirvanyants, N. Ermoshkin, R. Januszewicz, A. R. Johnson, D. Kelly, K. Chen, R. Pinschmidt, J. P. Rolland, A. Ermoshkin, E. T. Samulski, and J. M. DeSimone, Continuous liquid interface production of 3D objects, *Science* **347**, 1349 (2015).
- [56] S. F. S. Shirazi, S. Gharehkhani, M. Mehrali, H. Yarmand, H. S. C. Metselaar, N. Adib Kadri, and N. A. A. Osman, A review on powder-based additive manufacturing for tissue engineering: Selective laser sintering and inkjet 3D printing, *Sci. Technol. Adv. Mater.* **16**, 033502 (2015).
- [57] K. Zhao and T. G. Mason, Assembly of colloidal particles in solution, *Rep. Prog. Phys.* **81**, 126601 (2018).
- [58] D. S. Wiersma, Disordered photonics, *Nat. Photonics* **7**, 188 (2013).
- [59] S. Martis, É. Marcotte, F. H. Stillinger, and S. Torquato, Exotic ground states of directional pair potentials via collective-density variables, *J. Stat. Phys.* **150**, 414 (2013).
- [60] S. Torquato, Hyperuniformity and its generalizations, *Phys. Rev. E* **94**, 022122 (2016).